J. Bangladesh Acad. Sci. 45(2); 217-229: December 2021 DOI: 10.3329/jbas.v45i2.56023

Journal of Bangladesh Academy of Sciences

Journal homepage: http://www.bas.org.bd/publications/jbas.html

Research Article

A comparative study of spin magnetic moment, spin polarization and Curie temperature of Heusler type compounds ($A_{2-x-y}Z_y$)MnZ (A = Ni, Pd, Pt and Z = Sb, Sn)

Mohammad Shahjahan*, Sagar Chandra Roy and Md. Jafrul Sadique

Department of Physics, University of Dhaka, Dhaka, Bangladesh

ARTICLE INFO

Article History

Received: 04 November 2021
Revised: 22 November 2021
Accepted: 23 November 2021

Keywords: Heusler compounds; $C1_b$ structure; $L2_1$ structure; Magnetic moment; Spin polarization; Curie temperature

ABSTRACT

The Heusler type compounds ($A_{2-x-y}Z_y$)MnZ (A = Ni, Pd, Pt; Z = Sb, Sn; x = 1, 0; and y = 0, antisite defects of Z atoms) are investigated to understand the induced magnetic properties. The structural phases $C1_b$ type half Heusler (x = 1, y = 0) compounds AMnZ and the corresponding $L2_1$ type full Heusler (x = y = 0) compounds A_2MnZ and some disordered compounds ($A_{1-y}Z_y$)MnZ and ($A_{2-y}Z_y$)MnZ (y = 0.01, 0.05) were calculated using the Korringa-Kohn-Rostoker Green's function method. The antisite doping of 1% (5%) Sb retained (suppressed) the half metallicity at ($Ni_{1-y}Sb_y$)MnSb, whereas the other compounds were found to be gapless in both spin directions. The density of states at the Fermi level exhibits the explicit spin polarization in the compounds. The net magnetic moments of the compounds are closer in their values, wherein the manganese atom is responsible for the major contribution to the magnetic moments, which is much larger than the partial moment of the other constituents. The Curie temperature (T_C) of the ordered ferromagnetic compounds was estimated using the mean-field approximation. The T_C higher than the room temperature was found for the ordered compounds, except for the cases of Pt_2MnSb and Pt_2MnSn. No literature value of T_C has been reported yet for these two compounds. Calculated spin moments and T_C agree well with the experimental results, where available.

Introduction

The Heusler type intermetallic compounds ($A_{2-x-y}Z_y$) MnZ (A = Ni, Pd, Pt, and Z = Sb, Sn) have drawn the attention of the metallurgist because of their promising technological applications (Webster, 1969; Campbell, 1975; Yu et al., 2015). The collinear magnetic and half-metallic behavior with noticeably high Curie temperature (T_C) and magneto-mechanical properties made these materials unique. The magnetic shape memory effect, large strain-induced changes in the magnetization, and field-induced super elasticity are also found in Heusler materials (Kulkova et al., 2006). It is desirable to have a magnetic shape memory alloy with the T_C higher than the room temperature (RT). The saturation magnetic moment and T_C are very much dependent on the composition of Heusler compounds. Since Heusler materials exhibit most of the properties of metals but have the structure of ordered like compounds, several different magnetic exchange mechanisms play a role in these. There are two major classes of Heusler materials with

*Corresponding author: <mjahan@du.ac.bd>

compositions AMnZ (x = 1, y = 0) treated as half Heusler (HH) compounds and A_2MnZ (x = y = 0) termed as full Heusler (FH) compounds, where A (Ni, Pd, Pt) and Mn are transition metal (TM) atoms and Z (Sb, Sn) denotes primary group atom. Heusler compounds were first studied in 1903 by F. Heusler (Heusler, 1903), who reported that it was possible to make ferromagnetic (FM) compounds from the non-FM constituents. He found the FM property in many of the compounds, although neither of the constituents was FM at all. Since then, these alloys have been studied theoretically and experimentally to predict new featured magnetic materials. The magnetic properties of these compounds are sensitive to the local geometry, chemical composition, and the ordering of the manganese atoms in the face centered cubic (FCC) sub-lattices. In 1983, de Groot and his coworkers (de Groot et al., 1983, 1984) had shown in their revolutionary studies that these materials belong to a novel class half metal, which has been since then investigated rigorously. By this time, some other interesting properties of Heusler compounds have been pointed out by different research groups (Elphick et al., 2021; Yu et al., 2015; Wu et al., 2020).

Recently, the Luo group investigated the electronic structures and magnetic properties of the HH compounds and predicted NiCrAl, NiCrGa, and NiCrIn as possible half metals with an energy gap in the minority spin direction and full spin polarization at the Fermi level (Luo et al., 2008). The Kaneko group had measured the pressure effect on the Curie point of FH compounds Ni_2MnSn and Ni_2MnSb with the pressure coefficient as $1.6x10^{-3}$ k bar^{-1} and $9x10^{-3}$ k bar^{1}, respectively (Kaneko et al., 1981). In the advent of spintronics, these materials become attractive because the half-metallic behavior is of prime interest to the metallurgist. In spintronic devices, spin-dependent electronic transport can be used to encode information by changing finite resistance through these magnetic half metals. These devices show increased integration densities, non-volatility of information, high-speed data processing, and reduced energy consumption than conventional semiconductor electronics. Strictly speaking, this type of transport with spin degrees of freedom has superseded the traditional semiconductor technologies.

Structurally, the HH and FH compounds belong to the $C1_b$- and $L2_1$-type phases, respectively, with the FCC sub-lattices in the unit cell (Hirohata et al., 2006). These materials can be FM, ferrimagnetic, antiferromagnetic, and nonmagnetic, depending on the conduction electron concentration and chemical bonding. Therefore, greater interests have grown in the in-depth study of the magnetic interactions present in these materials. In most Heusler compounds, Mn is the primary moment-carrying atom. The presence of localized spins (magnetic ions) of the *d* electrons of A and Mn atoms, an indirect RKKY (Ruderman-Kittel-Kasuya-Yosida) type exchange interaction plays a role in the origin of magnetic anisotropy of the system (Skomski et al., 2006). The second-order perturbation theory attains the exchange mediated by electron or hole states from the hybridized states.

This article is aims to realize the FM and half-metallic treatment in Heusler type disordered compounds. A comparative study of electronic and spin-polarized properties of the Heusler type twenty-four compounds $(A_{2-x-y}Z_y)MnZ$ (A = Ni, Pd, Pt; Z = Sb, Sn; x = 1, 0; and y = 0, antisite defects of Z atoms) are investigated to explain the induced magnetic properties. The antisite doping of 1% (5%) Sb retained (suppressed) the half-metallicity at $(Ni_{1-y}Sb_y)MnSb$. The magnetic moments and spin polarizations of the Heusler type compounds are calculated, whereas the T_C is estimated only for the ordered Heusler materials. Despite the closeness of the experimental magnetic moments for the ordered systems, their Curie temperatures appeared to differ strongly. Moreover, spin-resolved electronic density of states (DOS) is calculated to seek the underlying reasons for the induced partial moments, the polarity of moments, and polarized spin properties of the Heusler type compounds.

The layout of the article is as follows. The computational framework is briefly outlined in section 2. The results and discussion are sub-sectioned into three parts, namely magnetic moments, Curie temperature, and spin-resolved electronic DOS, which are explained in detail in section 3. The comparisons of the calculated values with the reported experimental results are summarized in Table 1 and Table 3. The moments of the disordered systems are assembled in Table 2 and Table 4, whereas their DOS are displayed in Figs. (3-6). Finally, the concluding remarks on the presented results are outlined in section 4.

Methods of Calculation

Spin polarization and collinear magnetic properties of Heusler type compounds were calculated using the KKR-Green's function method, where two magnetic states were calculated for two different spin orientations. The calculations were carried out within the formalism of scalar relativistic approximation by neglecting spin-orbit interactions. The generalized gradient approximation was used for the exchange-correlation functional of the potential scheme (Perdew et al., 1996a, 1996b). The muffin-tin (MT) potential approximation was used, where the MT radius was selected such that the potential spheres are mildly touched but non-overlap each other (Casula and Herman, 1983). The mean-field approximation (MFA) was used to calculate the T_C. In total 328 k points of the first Brillouin zone (BZ) were used to perform the BZ integration. We specify the quality of the BZ and obtain the number of k points, which is used for the irreducible part of the BZ integration, as an output parameter. The compounds were taken to be crystallized in the FCC structure. The Fig. 1(b) shows the $L2_1$ phase of FH compounds A_2MnZ, where two atomic coordinates of 'A' atoms are (0.25, 0.25, 0.25), (0.75, 0.75, 0.75), coordinates of Mn and Z atoms are Mn (0.5, 0.5, 0.5) and Z (0, 0, 0). For the case of the $C1_b$ phase of HH compounds AMnZ, one of the two sites of 'A' atoms becomes empty, as shown in Fig. 1(a). The accuracy of the $C1_b$ phase calculations was assured by filling the one vacant site with a dummy atom having zero nuclear charges. Lattice relaxation was neglected in the present analysis, instead that, considering the accuracy of the calculation, we have used an experimental lattice parameter (LP). Whenever experimental LP is unavailable, then we estimate it using the energy minimization technique (EMT) to induce minimum error. The experimental LP was used for the four HH (Youn and Min, 1995; Offernes et al., 2008; Hames, 1960) and one FH Ni_2MnSb (Hames, 1960) compound. Theoretical LP was used for two FH compounds, Pd_2MnSb (Webster and Tebble, 1968) and Pt_2MnSn (Roy and Chakrabarti, 2017). The LP of the FH compound Pt_2MnSb was estimated using the EMT, which lacks any experimental or theoretical values in the literature. The LP of the ordered compounds is directly used to calculate the disordered compounds. The software package 'Machikaneyama' 2011 (Akai, 2011) is used for numerical computations.

Results and Discussion

The material diplatinum manganese antimonide, Pt_2MnSb is a media for high-density magneto-optic memory systems. Its LP was estimated using the energy minimization scheme, as shown in Fig. 2(a), where the calculated ground state energy is plotted with respect to the LP. The parameter against minimum energy is opted from the graph, as indicated by the dashed lines. Then using the optimized LP, its collinear magnetic and electronic properties have been calculated. The investigated material is deemed FM and therefore, its magnetic critical temperature is calculated in comparison to the ground state energy of the corresponding disordered local moment (DLM) state. As far as we know, there is no report on the value of its LP, neither experimentally nor theoretically in the literature. This material exhibits FM properties with low T_C. Its FM stability can be explained by the RKKY type exchange interactions, which are schematically diagramed in Fig. 2(b) (Skomski et al., 2006). The non-localized conduction electron's spin interacts with the localized inner *d* electron spins and thus creating linear correlation energy between the spins. Therefore, the *d* electron spins are aligned through this interaction, thereby stabilizing the FM state.

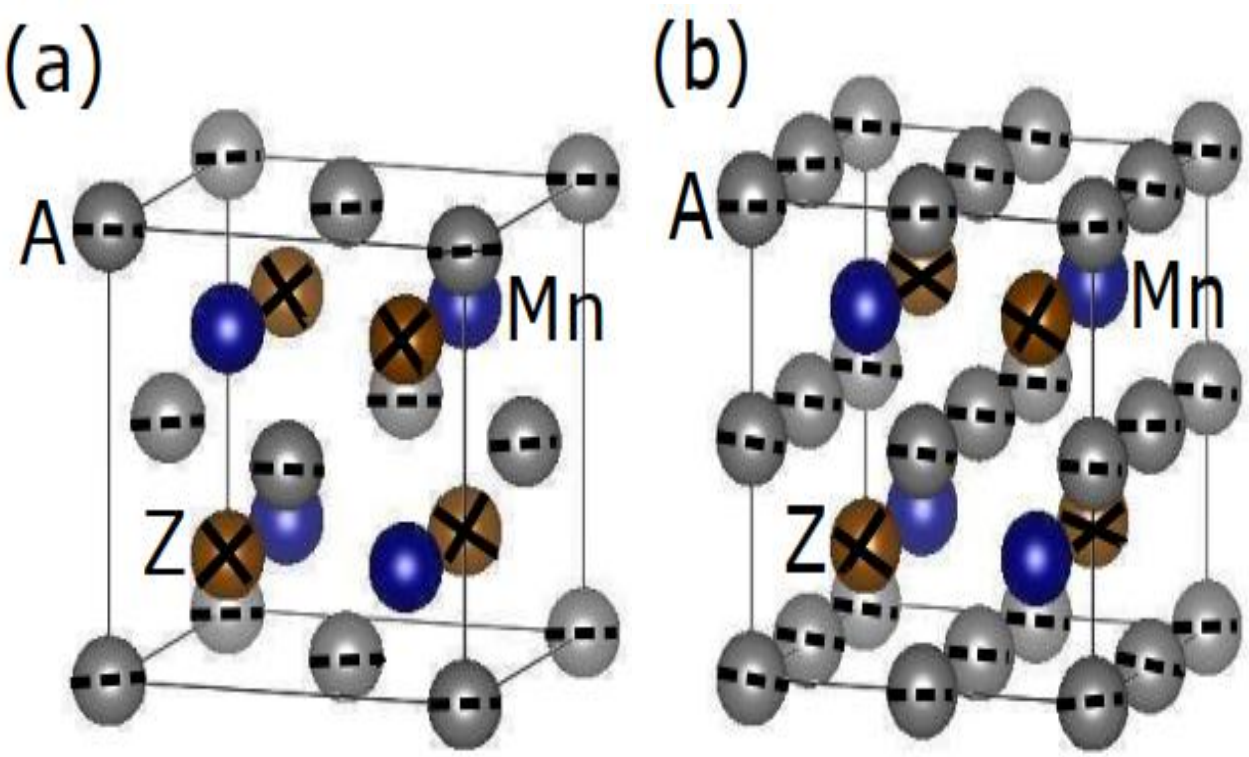

Fig. 1. The unit cell of (a) half Heusler and (b) full Heusler crystal structures with three and four atoms in the formula unit, respectively. Here A (Ni, Pd, Pt) implies transition metal atom, and Z (Sb, Sn) signifies primary (p) block atom.

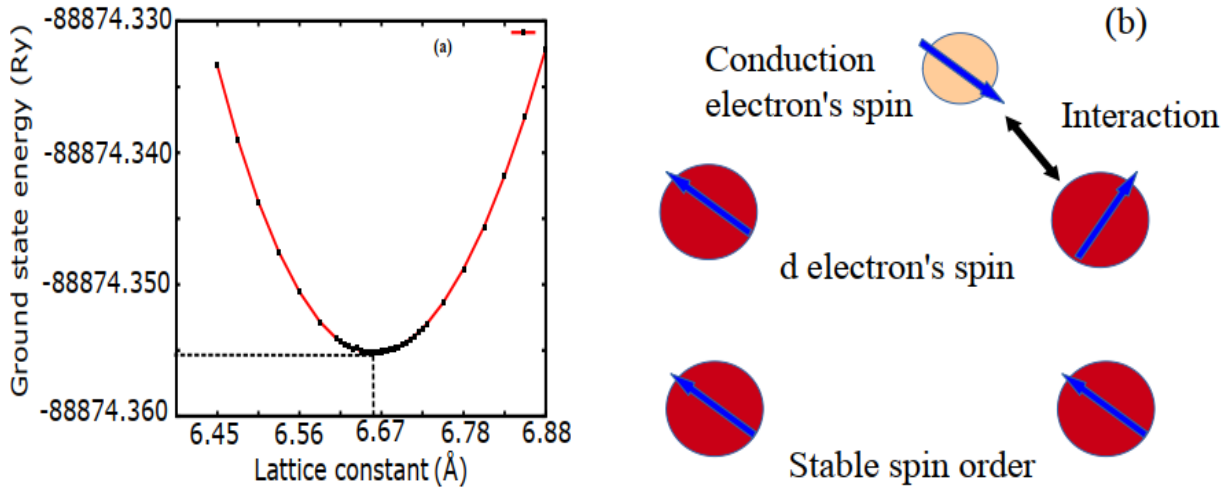

Fig. 2. (a) Calculated lattice parameter of a full Heusler compound Pt_2MnSb using the energy minimization technique, and (b) Schematic diagram of RKKY type exchange interaction, which makes the spin state stable.

Magnetic Moments

The magnetic moment represents the magnetic strength and orientation of a magnetic material resulting from the motion of electrons in atoms or the spin of the electrons. The saturated magnetic moments are calculated for four HH compounds, namely, NiMnSb, PdMnSb, PtMnSb, and PtMnSn, and eight HH-type compounds $(A_{1-y}Z_y)MnZ$ (y = 0.01, 0.05). The FM calculations were carried out for the compounds, where the saturated magnetic moment of each compound is found to be the sum of the local spin moments of the constituent atoms. The spin magnetic moment of an electron, an intrinsic property, is approximately one Bohr magneton, 1 μ_B. The spin magnetic moments of the constituent atoms are very low in strength compared to the spin magnetic moment of the Mn atom. However, in NiMnSb, the Mn site contains unoccupied minority bands, whereas the Ni site contains fully occupied bands in both spin polarization (Galanakis and Mavropoulos, 2007). As a result, the magnetic moment of the compound is localized at the Mn site. The net magnetic moments of the materials are mainly due to the spin moment at the Mn site. The cation sites of A and Mn in the formula AMnZ provide positive moments, whereas the Sb and Sn atoms at the Z site provide negative moments. In NiMnSb, PdMnSb, and PtMnSb, there are 22 valance electrons in each compound and 21 valence electrons in PtMnSn. Galanakis and others (Galanakis et al., 2002) show these materials to follow the moment rule $M_t = Z_t - 18$, where M_t is the total magnetic moment, and Z_t is the total number of valance electrons. The estimation of the magnetic moment for NiMnSb and PtMnSb exactly agrees with this rule since the calculated values of the moment are almost equal to 4 μ_B. Calculated total moment of the compounds is compared with the experimental results determined by van Engen and others (van Engen et al., 1983). The calculated values of the net moment are quite close to the measured values. The induced moments at vacancy and Z_y sites are negligible. The anion site (Z) moments are antiparallel to the moments at cation sites, as shown in Table 1 and Table 2.

Table 1. Lattice constant (a), partial and total magnetic moments, and Curie temperature of the half Heusler compounds $(A_{2-x-y}Z_y)MnZ$ (x = 1, y = 0). TM^{calc} (TM^{expt}) represents the total moment's calculated (experimental) values. The ΔE represents the energy difference between DLM and FM states. T_C^{calc} (T_C^{expt}) represents the calculated (experimental) values of Curie temperature. Here A and Z indicate the first and third atoms of the compounds AMnZ.

Materials	a (Å)	A (μ_B/atom)	Mn (μ_B/atom)	Z (μ_B/atom)	Vacancy (μ_B/atom)	TM^{calc} (μ_B/cell)	TM^{expt} (μ_B/cell)	ΔE (mRy)	T_C^{calc} (K)	T_C^{expt} (K)
NiMnSb	5.920	0.219	3.871	-0.110	0.008	4.001	3.85	11.6	1221	730
PdMnSb	6.250	0.078	4.189	-0.140	0.008	4.144	3.95	8.6	905	500
PtMnSb	6.210	0.096	4.091	-0.113	0.008	4.089	3.97	8.9	937	582
PtMnSn	6.264	0.049	4.082	-0.131	0.008	3.955	3.42	3.0	316	354

Table 2. Site projected partial and total magnetic moments per unit cell of the half Heusler type compounds ($A_{2-x-y}Z_y$)MnZ (x = 1, y = 0.01, 0.05). Here Z_y is the antisite doping at 1% and 5% atomic concentration of Z atoms. TM^{calc} represents the calculated values of the total moment. Here A and Z indicate the first and fourth atoms of the compounds ($A_{1-y}Z_y$)MnZ.

Materials	Z_y (μ_B/atom)	A (μ_B/atom)	Mn (μ_B/atom)	Z (μ_B/atom)	Vacancy (μ_B/atom)	TM^{calc} (μ_B/cell)
$(Ni_{0.99}Sb_{0.01})MnSb$	0.013	0.224	3.864	-0.090	0.008	4.049
$(Ni_{0.95}Sb_{0.05})MnSb$	0.013	0.298	3.908	-0.053	0.010	4.188
$(Pd_{0.99}Sb_{0.01})MnSb$	0.016	0.151	4.176	-0.134	0.007	4.179
$(Pd_{0.95}Sb_{0.05})MnSb$	0.020	0.179	4.175	-0.098	0.011	4.265
$(Pt_{0.99}Sb_{0.01})MnSb$	0.017	0.157	4.084	-0.123	0.008	4.096
$(Pt_{0.95}Sb_{0.05})MnSb$	0.029	0.198	4.108	-0.079	0.014	4.246
$(Pt_{0.99}Sn_{0.01})MnSn$	-0.047	0.125	4.143	-0.134	-0.011	3.996
$(Pt_{0.95}Sn_{0.05})MnSn$	-0.046	0.125	4.120	-0.131	-0.010	3.976

In addition to the HH compounds, the present work consists of four FH compounds such as Ni_2MnSb, Pd_2MnSb, Pt_2MnSb, and Pt_2MnSn, and eight FH type compounds ($A_{2-y}Z_y$)MnZ (y = 0.01, 0.05). The partial moments of the constituent atoms and the total moment of the compounds are listed in Table 3 and Table 4. Similar to the HH compounds, the magnetic moments of the FH compounds are mainly due to the contribution of the spin magnetic moment of the Mn atom. Neutron scattering experiments have verified that the magnetic moment of $L2_1$ type Heusler compounds resides mainly on the Mn site (Stearns, 1979). Kübler and others (Kübler et al., 1983) have explained that the origin of the magnetic moment is the localized nature of the electrons of Mn atoms within the compounds. However, a general rule for a magnetic moment in the FH compounds can be expressed as $M_t = Z_t - 24$, where M_t is the net magnetic moment, and Z_t is the total number of valance electrons. The Ni_2MnSb, Pd_2MnSb, and Pt_2MnSb compounds each have 32 valance electrons, and Pt_2MnSn has 31 valance electrons. Therefore, the moment rule for the cases of compounds with 32 and 31 valence electrons then predicts the moment value to be 8 μ_B and 7 μ_B, respectively. But the calculated magnetic moments retain in the range 4~4.5 μ_B. This fact can be explained as the paramagnetic effect of the Ni, Pd, and Pt atoms at position 'A' in the systems A_2MnZ. Due to their paramagnetic nature, these atoms fail to produce a large number of spin moments, and consequently, the net magnetic moment is much lower than the value predicted by the moment rule (Galanakis et al., 2002). Besides, the *d* electrons of Mn are itinerant, which originates the localization nature of *d* electron wave functions, and the spin-down electrons are almost excluded from the Mn site. The induced moments, in Table 4, at Z and Z_y sites are parallel, which together is oppositely oriented to the moments of cation sites.

Table 3. Lattice constant (a), partial and total magnetic moments, and Curie temperature of the full Heusler compounds ($A_{2-x-y}Z_y$)MnZ (x = y = 0). TM^{calc} (TM^{expt}) represents the total moment's calculated (experimental) values. The ΔE represents the energy difference between DLM and FM ground states. T_C^{calc} (T_C^{expt}) represents the calculated (experimental) values of Curie temperature. Here A_+ and A_{++} indicate the two atomic sites of 'A' atoms in the full Heusler compounds A_2MnZ, where Z indicates the third atom of the compounds.

Materials	a (Å)	A_+ (μ_B/atom)	A_{++} (μ_B/atom)	Mn (μ_B/atom)	Z (μ_B/atom)	TM^{calc} (μ_B/cell)	TM^{expt} (μ_B/cell)	ΔE (mRy)	T_C^{calc} (K)	T_C^{expt} (K)
Ni_2MnSb	6.001	0.154	0.154	3.691	-0.044	3.968	–	4.1	432	334
Pd_2MnSb	6.424	0.077	0.077	4.187	-0.042	4.308	4.40	3.4	358	247
Pt_2MnSb	6.660	0.127	0.127	4.313	-0.008	4.592	–	0.4	42	–
Pt_2MnSn	6.460	0.090	0.090	4.103	-0.023	4.264	–	1.7	179	–

Table 4. Site projected partial moments and total magnetic moments per unit cell of the full Heusler type compounds ($A_{2-x-y}Z_y$)MnZ (x = 0, y = 0.01, 0.05). Here Z_y is the antisite doping at 1% and 5% atomic concentrations of Z atoms. TM^{calc} represents the calculated values of the total moment. Here A_+ and A_{++} indicate the two atomic sites of 'A' atoms in the compounds ($A_{2-y}Z_y$)MnZ, where Z indicates the fourth atom of the compounds.

Materials	Z_y (μ_B/atom)	A_+ (μ_B/atom)	A_{++} (μ_B/atom)	Mn (μ_B/atom)	Z (μ_B/atom)	TM^{calc} (μ_B/cell)
$(Ni_{1.99}Sb_{0.01})MnSb$	-0.025	0.182	0.182	3.675	-0.058	3.942
$(Ni_{1.95}Sb_{0.05})MnSb$	-0.028	0.200	0.203	3.661	-0.051	3.951
$(Pd_{1.99}Sb_{0.01})MnSb$	-0.048	0.144	0.144	4.219	-0.045	4.364
$(Pd_{1.95}Sb_{0.05})MnSb$	-0.055	0.138	0.138	4.189	-0.047	4.319
$(Pt_{1.99}Sb_{0.01})MnSb$	-0.064	0.164	0.164	4.351	-0.010	4.518
$(Pt_{1.95}Sb_{0.05})MnSb$	-0.071	0.172	0.170	4.327	-0.005	4.522
$(Pt_{1.99}Sn_{0.01})MnSn$	-0.018	0.152	0.152	4.174	-0.027	4.319
$(Pt_{1.95}Sn_{0.05})MnSn$	-0.020	0.145	0.145	4.154	-0.027	4.283

Curie Temperature

The Curie temperature is the critical point when the magnetic moments change direction randomly, and the material loses its magnetic order. The resulting spin state of the paramagnetic material is regarded as the DLM state. Consequently, the energy difference ΔE between the FM and DLM states is calculated, which is the kernel parameter to estimate T_C. The expression $T_C = (2\Delta E)/(3k_B)$ is used to estimate the critical temperature of the Heusler compounds under consideration, where k_B is the Boltzmann constant. The estimated T_C with the available experimental values (Watanabe, 1975; Endo, 1970; Masumoto and Watanabe, 1972) is given in Table 1 and Table 3. Hames and Crangle (Hames and Crangle, 1971) have reported the experimental T_C for the PtMnSb to be 575 K and 330 K for the PtMnSn, which are closer to the values of the present calculation. The MFA often overestimates T_C in comparison to the experimental results, whereas the estimated T_C for PtMnSn is in good agreement with the experiments. The reason of the overestimation is that the framework of MFA does not include abruptness of spin within the compounds (Rusz et al., 2006; Majlis, 2007). However, the Rusz group (Rusz et al., 2006) have reported that the T_C for NiMnSb to be as high as 1106 K. Their calculation closely concurs with the presented result for the same compound. In addition, the estimated T_C of the compounds AMnZ (x = 1, y = 0) is found higher than the RT.

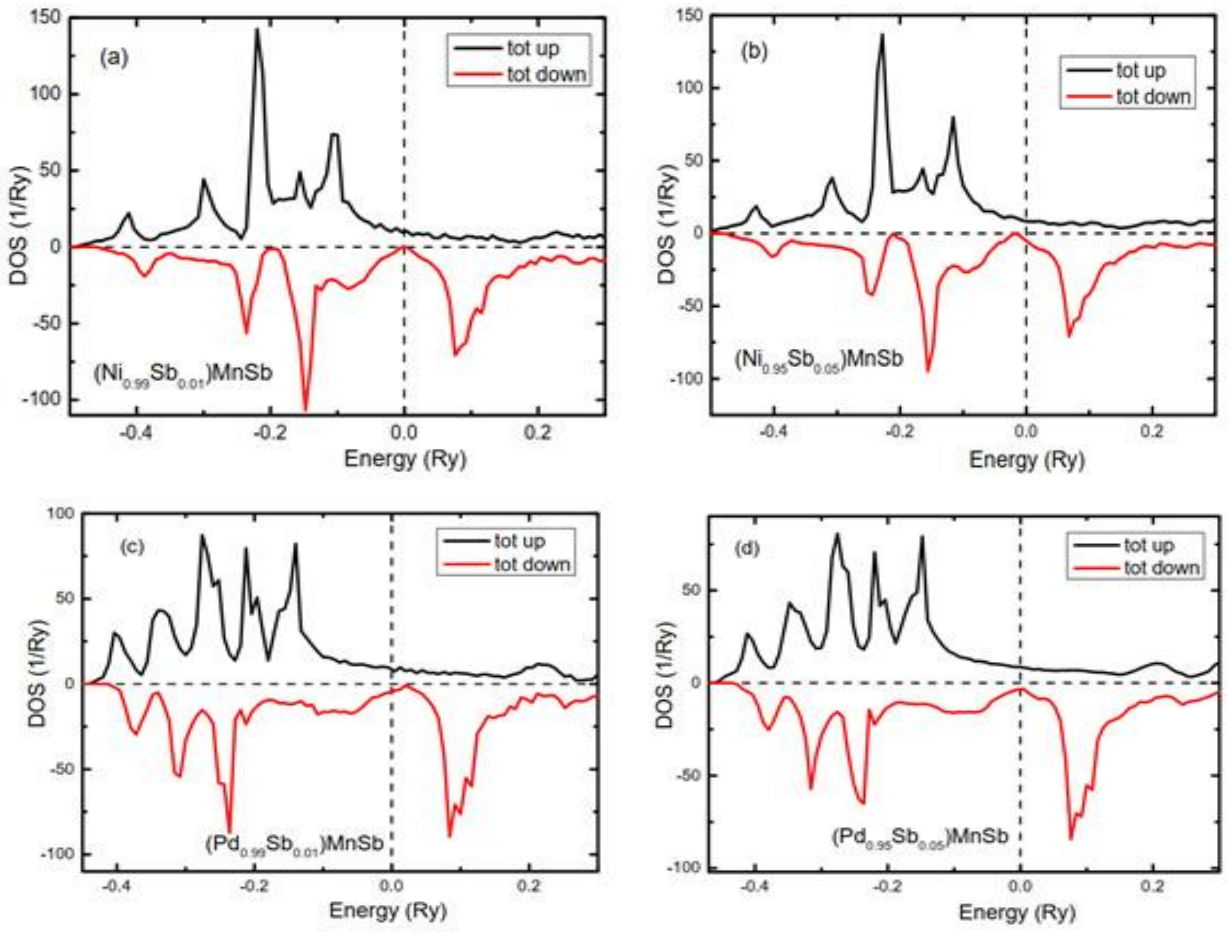

Fig. 3. The solid curves indicate the total DOS of (a) $(Ni_{0.99}Sb_{0.01})MnSb$, (b) $(Ni_{0.95}Sb_{0.05})MnSb$, (c) $(Pd_{0.99}Sb_{0.01})MnSb$, and (d) $(Pd_{0.95}Sb_{0.05})MnSb$ with 1% and 5% antisite doping of Sb atom. Vertical dashed lines are the Fermi energy level.

Moreover, the estimated T_C with the available experimental results for the FH compounds Ni_2MnSb (Kaneko et al., 1981) and Pd_2MnSb (Webster and Tebble, 1968), are shown in Table 3. For these two compounds, the T_C is found to be higher than the RT. There was no experimental T_C available for the compounds Pt_2MnSb and Pt_2MnSn. Using the MFA, Rusz et al. (Rusz et al., 2006) have reported that the T_C for Ni_2MnSb to be 575 K, higher than the RT. It should be noted that both the Pt content compounds exhibit a low T_C. Furthermore, it was assumed that the energy difference ΔE for a FH compound might be half of its HH counterpart. It is clear from Table 1 and Table 3 that this assumption is true at least approximately. However, one exception is noted for the case of Pt_2MnSb, which exhibits a quite smaller quantity. The underlying reason for this anomaly is that the partial moments of 'A' atoms are collinear with the same strength and arise basically from the two unoccupied minority conduction bands. Therefore, the two 'A' atoms together have a total moment of about 0.25 μ_B. In contrast, the *sp* atom has a very small negative moment (-0.008 μ_B) which is smaller in magnitude and oppositely oriented to the spin moments of 'A' atoms. The negative sign of the induced moment of primary group atom, belonging to the fifth row of the Periodic Table, is an exceptional characteristic of the Heusler compounds.

Spin Resolved Electronic Density of States (DOS)

The DOS of a system is described by the number of electronic states per energy interval of occupied or empty energy levels [E, E+dE]. Its quality requires very fine k-meshes of the irreducible part of the BZ, where 328 k points were used to calculate DOS. The spin-resolved electronic DOS of the HH type disordered compounds $(A_{1-y}Z_y)MnZ$ (y = 0.01, 0.05) are shown in Figs. 3(a-d) and Figs. 4(a-d). The KKR-Green's function calculation manifests that only $(Ni_{1-y}Sb_y)MnSb$ was found to be half-metallic, as shown in Fig. 3(a), which is reported in the literature for NiMnSb by de Groot et al. (de Groot et al., 1983) with augmented spherical wave method. In $(Ni_{1-y}Sb_y)MnSb$, the Mn site has only its majority bands occupied, leaving the minority bands unfilled, whereas Ni has both bands filled up. This phenomenon gives rise to the half-metallic behavior of $(Ni_{1-y}Sb_y)MnSb$ with full spin polarization at the majority band and a zero DOS (no states are available at that energy level) at the minority band. However, on the same footing, $(Pd_{1-y}Sb_y)MnSb$, $(Pt_{1-y}Sb_y)MnSb$, and $(Pt_{1-y}Sn_y)MnSn$ might show the half-metallic property. But in these compounds, in contrast to available theoretical predictions, we have found them to be FM rather than half-metallic. Still, these materials have a high value of spin polarization at the Fermi level. Due to the higher concentrations of antisite doping, spin states are prominently shifted towards the valence band, and the resulting spin polarization is FM in nature.

The spin-resolved DOS of the FH type disordered compounds $(A_{2-y}Z_y)MnZ$ (y = 0.01, 0.05) are gathered in Figs. 5(a-d) and Figs. 6(a-d). The DOS, a function of energy, is a continuous pattern of resolute electronic states in metal due to local potential, whereas the pattern discontinuity arises in half-metal. The valence band extends around the Fermi level, and the spin-split DOS shows a large peak below the Fermi level for these compounds. In the case of FH type compounds, each Mn atom has eight 'A' atoms as first neighbors instead of four as in the case of HH type compounds $(A_{1-y}Z_y)MnZ$. Therefore, the hybridization effect significantly decreases the Mn spin moment to less than 4 μ_B in the case of the compounds $(Ni_{2-y}Sb_y)MnSb$. The spin moments of 'A' atoms are ferromagnetically coupled to the Mn spin moment, and the materials possess a high spin polarization of the electronic states at the Fermi level. The higher antisite doping produces more antisite moment and shifting of electronic states, lying deeper in energy and thus stabilizing the FM state.

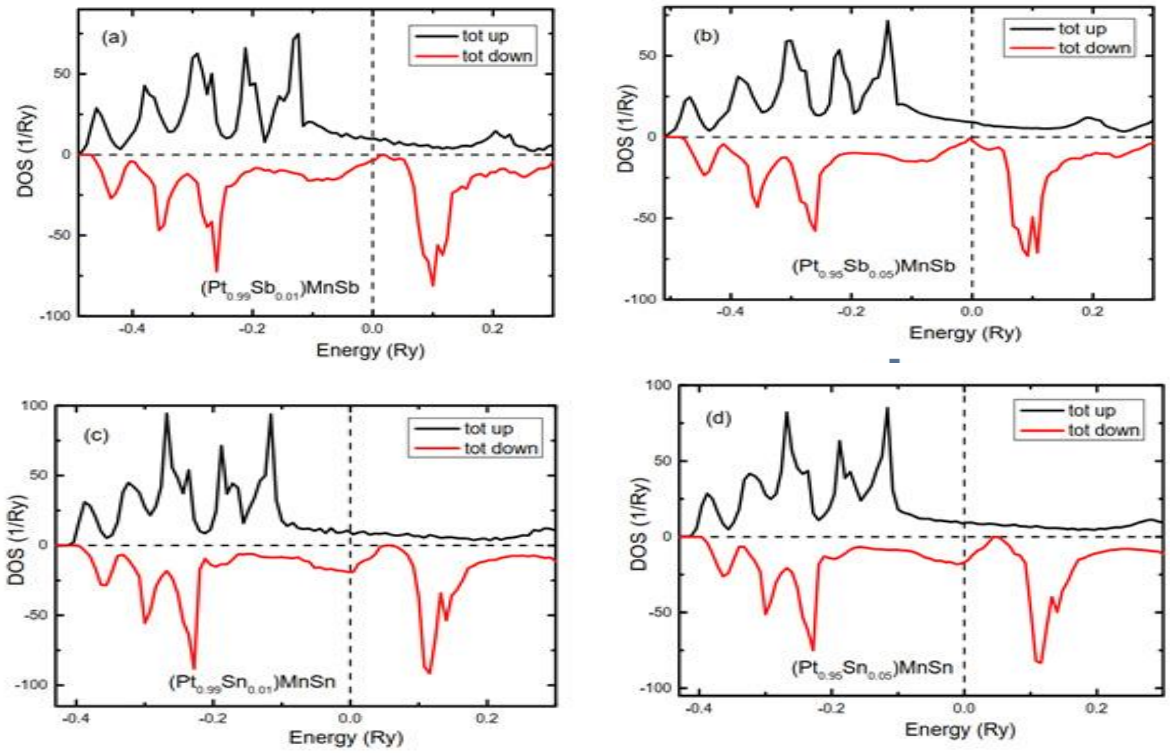

Fig. 4. The solid curves indicate the total DOS of (a) $(Pt_{0.99}Sb_{0.01})MnSb$, (b) $(Pt_{0.95}Sb_{0.05})MnSb$, (c) $(Pt_{0.99}Sn_{0.01})MnSn$, and (d) $(Pt_{0.95}Sn_{0.05})MnSn$ with 1% and 5% antisite doping of Sb and Sn atoms. Vertical dashed lines are the Fermi energy level.

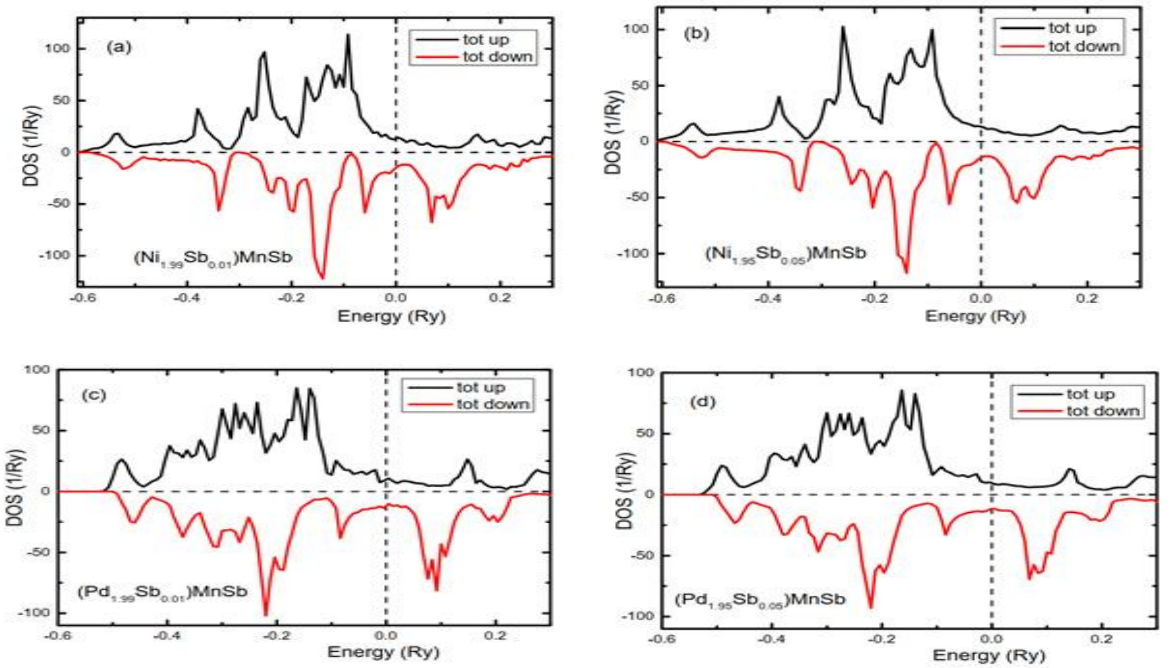

Fig. 5. The solid curves indicate the total DOS of (a) $(Ni_{1.99}Sb_{0.01})MnSb$, (b) $(Ni_{1.95}Sb_{0.05})MnSb$, (c) $(Pd_{1.99}Sb_{0.01})MnSb$, and (d) $(Pd_{1.95}Sb_{0.05})MnSb$ with 1% and 5% antisite doping of Sb atom. Vertical dashed lines are the Fermi energy level.

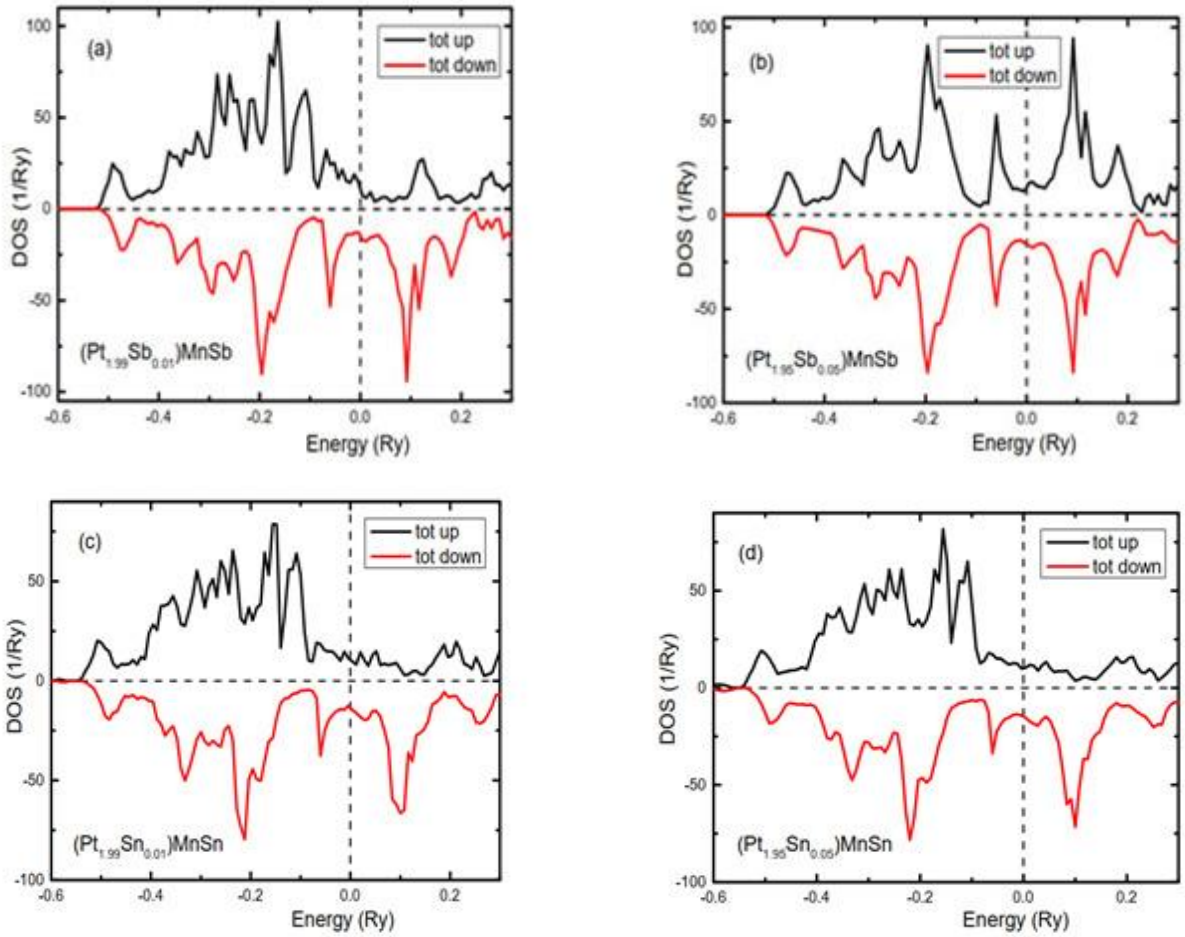

Fig. 6. The solid curves indicate the total DOS of (a) $(Pt_{1.99}Sb_{0.01})MnSb$, (b) $(Pt_{1.95}Sb_{0.05})MnSb$, (c) $(Pt_{1.99}Sn_{0.01})MnSn$, and (d) $(Pt_{1.95}Sn_{0.05})MnSn$ with 1% and 5% antisite doping of Sb and Sn atoms. Vertical dashed lines are the Fermi energy level.

Conclusion

Spin polarization and collinear magnetic properties have been investigated for Heusler type compounds $(A_{2-x-y}Z_y)MnZ$, using the KKR-Green's function approach, where spherically symmetric atomic sphere potentials construct the wave functions and charge densities. Extensive calculations show a large magnetic effect of Mn atom of the compounds. The magnetic moments are compared with the available experimental values, where the observed moments agree with the calculated results. The estimated values of T_C for the Heusler compounds are found higher than the RT, whereas only two of the four FH compounds exhibit low T_C.

The T_C is related proportionally to the spin density wave; that is, the higher spin density produces more T_C. The $(Ni_{1-y}Sb_y)MnSb$ with 1% antisite doping has retained the full spin-polarized charge injection for the application in the spintronic devices. The novel functional devices that control the charge of electrons and spin degrees of freedom are considered to be fabricated by emergent magnetic materials.

Acknowledgment

The present work was performed with the advanced computational facilities of the center for advanced research in sciences (CARS), University of Dhaka. The authors are thankful to CARS for the supports.

Conflicts of Interest

The authors declare that they have no conflicts of interest regarding the publication of this article.

References

Akai H. Ab initio electronic structure calculation code. 2011; http://kkr.issp.u-tokyo.ac.jp.

Campbell CCM. Hyperfine field systematics in Heusler alloys. *J. Phys. F: Met. Phys.* 1975; 5(10): 1931-1945.

Casula F and Herman F. Generalized muffin-tin orbitals for electronic structure studies of surfaces, interfaces, and organic solids. *J. Chem. Phys*. 1983; 78(2): 858–875.

de Groot RA, Mueller FM, van Engen PG and Buschow KHJ. New class of materials: half-metallic ferromagnets. *Phys. Rev. Lett*. 1983; 50(25): 2024-2027.

de Groot RA, Mueller FM, van Engen PG and Buschow KHJ. Half-metallic ferromagnets and their magneto-optical properties. *J. Appl. Phys*. 1984; 55(6): 2151-2154.

Endo K. Magnetic studies of Cl_b-compounds CuMnSb, PdMnSb and Cu_{1-x}(Ni or Pd)$_x$MnSb. *J. Phys. Soc. Jpn*. 1970; 29(3): 643-649.

Elphick K, Frost W, Samiepour M, Kubota T, Takanashi K, Sukegawa H, Mitani S and Hirohata A. Heusler alloys for spintronic devices: review on recent development and future perspectives. *Sci. Technol. Adv. Mater*. 2021; 22(1): 235-271.

Galanakis I and Mavropoulos P. Spin-polarization and electronic properties of half-metallic Heusler alloys calculated from first principles. *J. Phys. Condens. Matter* 2007; 19(31): 315213-315228.

Galanakis I, Dederichs PH and Papanikolaou N. Origin and properties of the gap in the half-ferromagnetic Heusler alloys. *Phys. Rev. B* 2002; 66(13): 134428-134437.

Heusler F. Über magnetische manganlegierungen. *Verh. Dtsch. Phys. Ges*. 1903; 5(12): 219.

Hirohata A, Kikuchi M, Tezuka N, Inomata K, Claydon JS, Xu YB and van der Laan G. Heusler alloy/semiconductor hybrid structures. *Curr. Opin. Solid State Mater. Sci*. 2006; 10(2): 93-107.

Hames FA. Ferromagnetic-alloy phases near the compositions Ni_2MnIn, Ni_2MnGa, Co_2MnGa, Pd_2MnSb, and PdMnSb. *J. Appl. Phys*. 1960; 31(5): S370-S371.

Hames FA and Crangle J. Ferromagnetism in Heusler-type alloys based on platinum-group or palladium-group metals. *J. Appl. Phys*. 1971; 42(4): 1336-1338.

Kulkova SE, Eremeev SV, Kakeshita T, Kulkov SS and Rudenski GE. The electronic structure and magnetic properties of full- and half-Heusler alloys. *Materials Transactions*, 2006; 47(3): 599-606.

Kaneko T, Yoshida H, Abe S and Kamigaki K. Pressure effect on the Curie point of the Heusler alloys Ni_2MnSn and Ni_2MnSb. *J. Appl. Phys*. 1981; 52(3): 2046-2048.

Kübler J, William AR and Sommers CB. Formation and coupling of magnetic moments in Heusler alloys. *Phys. Rev. B* 1983; 28(4): 1745-1755.

Luo H, Zhu Z, Liu G, Xu S, Wu G, Liu H, Qu J and Li Y. Ab initio investigation of electronic properties and magnetism of half-Heusler alloys XCrAl (X = Fe, Co, Ni) and NiCrZ (Z = Al, Ga, In). *Physica B: Condens. Matter*. 2008; 403(1): 200-206.

Masumoto H and Watanabe K. On magnetic properties of intermetallic fluorite-type compound PtMnSn in the Pt-Mn-Sn system. *J. Jpn. Inst. Met. Mater*. 1972; 36(9): 827-833.

Majlis N. The q*uantum theory of magnetism. 2nd ed. World scientific, New Jersey, U.S.A.*; 2007; p. 62.

Offernes L, Ravindran P, Seim CW and Kjekshus A. Prediction of composition for stable half-Heusler phases from electronic-band-structure analyses. *J. Alloys Compd*. 2008; 458(1-2): 47-60.

Perdew JP, Burke K and Ernzerhof M. Generalized gradient approximation made simple. *Phys. Rev. Lett*. 1996a; 77(18): 3865-3868.

Perdew JP, Burke K and Wang Y. Generalized gradient approximation for the exchange-correlation hole of a many-electron system. *Phys. Rev. B* 1996b; 54(23): 16533-16539.

Roy T and Chakrabarti A. Ab initio study of effect of Co substitution on the magnetic properties of Ni and Pt-based Heusler alloys. *Phys. Lett. A* 2017; 381(16): 1449-1456.

Rusz J, Bergqvist L, Kudrnovský J and Turek I. Exchange interactions and Curie temperatures in Ni_{2-x} MnSb alloys: First-principles study. *Phys. Rev. B* 2006; 73(21): 214412-214421.

Skomski R, Zhou J, Zhang J and Sellmyer DJ. Indirect exchange in dilute magnetic semiconductors. *J. Appl. Phys*. 2006; 99(8): 08D504-08D506.

Stearns MB. Hyperfine field and magnetic behavior of Heusler alloys. *J. Appl. Phys*. 1979; 50(B3): 2060-2062.

van Engen PG, Buschow KHJ, Jongebreur R and Erman M. PtMnSb, a material with very high magneto-optical Kerr effect. *Appl. Phys. Lett*. 1983; 42(2): 202-204.

Webster PJ. Heusler alloys. *Contemp. Phys*. 1969; 10(6): 559-577.

Webster PJ and Tebble RS. Magnetic and chemical order in Pd_2MnAl in relation to order in the Heusler alloys Pd_2MnIn, Pd_2MnSn, and Pd_2MnSb. *J. Appl. Phys*. 1968; 39(2): 471-474.

Watanabe K. Magnetic properties of Mn base $C1_b$-type compounds. *J. Jpn. Inst. Metals Mater*. 1975; 39(5): 498-502.

Wu M, Zhou F, Khenata R, Kuang M and Wang X. Phase transition and electronic structures of all-*d*-metal Heusler-type X_2MnTi compounds (X = Pd, Pt, Ag, Au, Cu, and Ni). *Front. Chem.* 2020; 8: 546947-546957.

Yu GH, Xu YL, Liu ZH, Qiu HM, Zhu ZY, Huang XP and Pan LQ. Recent progress in Heusler-type magnetic shape memory alloys. *Rare Met.* 2015; 34(8): 527-539.

Youn SJ and Min BI. Effects of the spin-orbit interaction in Heusler compounds: electronic structures and Fermi surfaces of NiMnSb and PtMnSb. *Phys. Rev. B* 1995; 51(16): 10436-10442.